

Control of Surface Chemistry, Substrate Stiffness, and Cell Function in a Novel Terpolymer Methacrylate Library

Abraham Joy,^{†,§} Daniel M. Cohen,[‡] Arnold Luk,[†] Emmanuel Anim-Danso,[†] Christopher Chen,[‡] and Joachim Kohn^{*†}

[†]New Jersey Center for Biomaterials and Department of Chemistry and Chemical Biology, Rutgers University, Piscataway, New Jersey 08854, United States, and [‡]Department of Bioengineering, University of Pennsylvania, Philadelphia, Pennsylvania 19104, United States. [§]Current Address: Department of Polymer Science, The University of Akron, Akron, OH 44325.

Received September 17, 2010. Revised Manuscript Received November 24, 2010

A focused library of methacrylate terpolymers was synthesized to explore the effects of varying surface chemistry and adhesive peptide ligands on cell function. The chemical diversity of methacrylate monomers enabled construction of a library of polymers in which one can systematically vary the chemical composition to achieve a wide range of contact angle, Young's modulus, and T_g values. Furthermore, the materials were designed to allow surface immobilization of bioactive peptides. We then examined the effects of these material compositions on protein adsorption and cell attachment, proliferation, and differentiation. We observed that chemical composition of the polymers was an important determinant for NIH 3T3 cell attachment and proliferation, as well as human mesenchymal stem cell differentiation, and correlated directly with the ability of the polymers to adsorb proteins that mediate cell adhesion. Importantly, functionalization of the methacrylate terpolymer library with an adhesive GRGDS peptide normalized cellular responses. RGD-functionalized polymers uniformly exhibited robust attachment, proliferation, and differentiation irrespective of the underlying substrate chemistry. These studies provide a library-based approach to rapidly explore the biological functionality of biomaterials with a wide range of compositions and highlight the importance of cell and protein cell adhesion in predicting their performance.

Introduction

A number of materials used in bioengineering applications are designed to emulate the properties of the extracellular matrix (ECM) to recapitulate cellular functions. The interaction of cells with the ECM regulates a number of physiological functions by providing both a structural support for cell growth and organization and by engaging adhesion receptors that initiate signal transduction.^{1–3} Designing the next generation of biomaterials requires an improved understanding of how material properties affect cellular behavior and the methodology to incorporate biologically relevant properties into biomaterials.^{4,5}

Cellular functions are modulated by a number of material properties, and currently, considerable effort is being directed at controlling cell functions by the use of designed materials.⁶ For example, the role of surface chemistry in controlling various cell functions is well appreciated. Self-assembled monolayers (SAMs) of different chemistry can influence the expression levels of osteoblast-specific marker proteins such as alkaline phosphatase

and bone sialoprotein during the differentiation of MC3T3 cells to osteoblasts.⁷ One approach to overcome the limitations of specific material compositions and their effects on cells is to couple adhesive peptides and ECM proteins onto materials to increase cell attachment and functional behavior of cells. Two decades ago, RGD was identified as a sufficient motif for fibronectin,⁸ and when conjugated to materials the RGD sequence increases cell attachment and viability.⁹ In addition to RGD, a number of peptide sequences have been identified that enable the adhesion and proliferation of specific cells.¹⁰ Besides surface chemistry, the mechanical strength and modulus of such materials are critical for the stability of many medical implant applications, and furthermore certain narrow ranges of stiffness have been implicated in modulating cellular functions such as cell motility and differentiation.^{11–13} Third, the amount or geometry of the ECM can play a crucial role in cellular responses, especially as it pertains to regulation of cell adhesion and spreading. Microfabricated

*To whom correspondence should be addressed. E-mail: kohn@rutgers.edu. Tel: 732-445-0488. Fax: 732-445-5006.

(1) Geiger, B.; Bershadsky, A.; Pankov, R.; Yamada, K. M. Transmembrane crosstalk between the extracellular matrix–cytoskeleton crosstalk. *Nat. Rev. Mol. Cell Biol.* **2001**, 2(11), 793–805.

(2) Romer, L. H.; Birukov, K. G.; Garcia, J. G. Focal adhesions: paradigm for a signaling nexus. *Circ. Res.* **2006**, 98(5), 606–16.

(3) Dubash, A. D.; Menold, M. M.; Samson, T.; Boulter, E.; Garcia-Mata, R.; Doughman, R.; Burrige, K. Chapter 1. Focal adhesions: new angles on an old structure. *Int. Rev. Cell Mol. Biol.* **2009**, 277, 1–65.

(4) Place, E. S.; Evans, N. D.; Stevens, M. M. Complexity in biomaterials for tissue engineering. *Nat. Mater.* **2009**, 8(6), 457–70.

(5) Lutolf, M. P.; Hubbell, J. A. Synthetic biomaterials as instructive extracellular microenvironments for morphogenesis in tissue engineering. *Nat. Biotechnol.* **2005**, 23(1), 47–55.

(6) Hench, L. L.; Polak, J. M. Third-generation biomedical materials. *Science* **2002**, 295(5557), 1014–7.

(7) Keselowsky, B. G.; Collard, D. M.; Garcia, A. J. Integrin binding specificity regulates biomaterial surface chemistry effects on cell differentiation. *Proc. Natl. Acad. Sci. U.S.A.* **2005**, 102(17), 5953–7.

(8) Pierschbacher, M. D.; Ruoslahti, E. Cell attachment activity of fibronectin can be duplicated by small synthetic fragments of the molecule. *Nature* **1984**, 309(5963), 30–3.

(9) Hersel, U.; Dahmen, C.; Kessler, H. RGD modified polymers: biomaterials for stimulated cell adhesion and beyond. *Biomaterials* **2003**, 24(24), 4385–415.

(10) Shin, H.; Jo, S.; Mikos, A. G. Biomimetic materials for tissue engineering. *Biomaterials* **2003**, 24(24), 4353–64.

(11) Engler, A. J.; Sen, S.; Sweeney, H. L.; Discher, D. E. Matrix elasticity directs stem cell lineage specification. *Cell* **2006**, 126(4), 677–689.

(12) Banerjee, A.; Arha, M.; Choudhary, S.; Ashton, R. S.; Bhatia, S. R.; Schaffer, D. V.; Kane, R. S. The influence of hydrogel modulus on the proliferation and differentiation of encapsulated neural stem cells. *Biomaterials* **2009**, 30(27), 4695–9.

(13) Lo, C. M.; Wang, H. B.; Dembo, M.; Wang, Y. L. Cell movement is guided by the rigidity of the substrate. *Biophys. J.* **2000**, 79(1), 144–52.

substrates that confine cells to ECM islands of specific areas, control whether endothelial cells proliferate or die, and whether mesenchymal stem cells (MSCs) differentiate to adipocytes versus osteoblasts.¹⁴ These elegant studies highlight the effect of one material property when examined in isolation from other physical parameters. However the cellular response to a synthetic biomaterial comprises the net effect of all the material properties and it is important to understand how and whether these properties coordinately regulate cellular adhesion to trigger a phenotypic response.

To begin to explore the large space parameters that impact the interplay of surface chemistry, substrate modulus, and cell adhesion, and their effects on cellular responses to biomaterials, one must consider alternative approaches to traditional, one-by-one comparisons of materials. Combinatorial libraries have been used successfully in the pharmaceutical industry for the exploration of a chemical space and identification of lead compounds.¹⁵ Currently, such libraries are being adapted for use in the polymer science field.^{16,17} Paired with computational modeling, these libraries present a potentially efficient method to shorten the time from concept to product.¹⁸ As such, combinatorial libraries of biomaterials may lay the foundation for the future development of bioresponsive medical devices.

In the current work, a focused library of methacrylate polymers was synthesized based on the rationale that changes in monomer composition will alter the physical and mechanical properties of polymers and potentially also influence the cellular responses. Correlating such changes in cell behavior to the changes in chemical composition across the library would provide a better understanding of how to program the cellular response to biomaterials. The focused polymer library was synthesized from a diverse set of methacrylate or acrylate monomers and by incorporation of a reactive monomer, these materials were efficiently surface functionalized with the RGD peptide, enabling the investigation of RGD-dependent responses in the context of a diverse library of polymers. The tunable features of the materials developed here enables the examination of how the substrate chemistry, compliance, and surface-grafted adhesive peptides act in concert to affect a variety of cellular functions, including cell attachment, proliferation, and differentiation.

Experimental Section

Materials and Methods. The monomers hydroxyethyl methacrylate (ophthalmic grade) (HEMA), 2-ethylhexyl acrylate (EHA), triethyleneglycol monomethylether monomethacrylate (TEGMA), *N*-isopropylacrylamide (NIPAAm), glycidyl methacrylate (GMA), and azobisisobutyronitrile (AIBN) were purchased from either Sigma-Aldrich or Polysciences and used as received.

N₃-PEG7-GRGDS peptide was custom synthesized by coupling an azido-PEG-acid to the N-terminus of amide protected GRGDS. The synthesis and purification was carried out by Twentyfirst Century Biochemicals, Inc. (Marlboro, MA). N₃-PEG-OMe (*M_w* 2000) was purchased from Sigma-Aldrich. Alexafluor 488 was obtained from Invitrogen (Carlsbad, CA). Fetal bovine serum was purchased from Gibco, fibrinogen from EMD Chemicals, and bovine serum albumin from Sigma-Aldrich.

(14) McBeath, R.; Pirone, D. M.; Nelson, C. M.; Bhadriraju, K.; Chen, C. S. Cell shape, cytoskeletal tension, and RhoA regulate stem cell lineage commitment. *Dev. Cell* **2004**, 6(4), 483–95.

(15) Lipinski, C.; Hopkins, A. Navigating chemical space for biology and medicine. *Nature* **2004**, 432(7019), 855–61.

(16) Brocchini, S.; James, K.; Tangpasuthadol, V.; Kohn, J. A combinatorial approach for polymer design. *J. Am. Chem. Soc.* **1997**, 119, 4553–4554.

(17) Hook, A. L.; Anderson, D. G.; Langer, R.; Williams, P.; Davies, M. C.; Alexander, M. R. High throughput methods applied in biomaterial development and discovery. *Biomaterials* **2010**, 31(2), 187–98.

(18) Kohn, J.; Welsh, W. J.; Knight, D. A new approach to the rationale discovery of polymeric biomaterials. *Biomaterials* **2007**, 28(29), 4171–7.

Synthesis and Purification of Polymers. The polymers were synthesized by AIBN-initiated radical polymerization of the three monomers in DMF at 70 °C. A typical reaction such as the synthesis of 40%HEMA-co-35%TEGMA-co-25%GMA was carried out as follows: HEMA (0.78 mL, 0.006 mols), TEGMA (1.29 mL, 0.005 mols), GMA (0.53 mL, 0.004 mols), and AIBN (2.5 mg, 0.015 mmol) were taken in a round bottomed flask. (The total monomer concentration was 0.015 mol.) Dimethylformamide (DMF) (12 mL) was added and the reaction was purged by a stream of nitrogen. The reaction was heated at 70 °C for 6 h with rapid stirring. The polymer was precipitated in diethyl ether. The obtained polymer was redissolved and precipitated (two more times) after which the polymer was dried for 2 days under vacuum.

Single Letter Notation for Monomers and Abbreviation of Polymer Composition

- Hydroxyethyl methacrylate = H
- Triethyleneglycol monomethylether monomethacrylate = T
- 2-Ethylhexyl acrylate = A
- *N*-isopropylacrylamide = N
- Glycidyl methacrylate = G
- H40T35G25 indicates a polymer composed of 40% H, 35% T, and 25% G (mole %).

Characterization of Polymers. The polymers were characterized by ¹H NMR (400 MHz; DMSO-*d*₆). The composition of the polymer was obtained by integration of peaks at 3.9 ppm (HEMA), 3.72 ppm (NIPAAm), 2.65 ppm (GMA), 1.57 ppm (EHA), and 3.65 ppm (TEGMA).

Molecular weights were determined by GPC (DMF or THF) using polystyrene standards.

The glass transition temperature (*T_g*) was determined by differential scanning calorimetry (2910 Modulated DSC, TA Instruments).

Tensile Testing. Thin (100 μm) polymer films were tested according to ASTM standard D882-91 on a Sintech 5/D tensile tester. Measurements were made with hydrated samples at room temperature after incubation in deionized water for 2 h and the results were averaged over three replicates. The width (5 mm) and thickness of each of the specimens tested were averaged over three measurements in different parts of each specimen. The displacement rate was 2 mm/min allowing for a reliable measurement of the tensile modulus.

Spin Coating of Polymers on Glass Coverslips. Glass coverslips were cleaned by sonicating them in a wide beaker (to prevent the coverslips from clumping together) first in acetone and then in ethanol. Individual coverslips then taken out of the ethanol and were dried under a strong stream of N₂ in a lint free environment, making sure that each coverslip was spot/debris free.

The polymers were spin coated from 1% solutions of the polymers in tetrahydrofuran (THF). For the polymers composed of higher amounts of HEMA, up to 8% methanol was added to the total volume of THF to ensure dissolution of the polymer. The polymers were spin coated (4000 rpm for 30 s) onto cleaned glass coverslips.

Contact Angle Measurements. Contact angle measurements were carried out on a Ramé-Hart goniometer equipped with a camera and DropImage software to measure the contact angle. The polymer-coated coverslips were incubated in PBS for 2 h prior to the measurements. A drop of deionized water was placed on the coverslip and the contact angle measured within 1–3 s. Similar procedure was followed for the polymer-coated coverslips functionalized with GRGDS peptide.

Surface Functionalization. For cell biology experiments, polymer-coated coverslips were used. These were surface functionalized using a two step procedure. First the surface epoxide groups of GMA were converted to surface propargyl groups by reaction with propargyl amine (1% solution in water) over a period of 18 h and then the coverslips were washed with water (3×) to remove any unreacted propargyl amine. In the second step, the surface propargyl groups were coupled to the N₃-PEG7-GRGDS peptide

by the Huisgen 1,3-cycloaddition reaction (Sharpless Click reaction conditions). The reagent was prepared by mixing 0.5 mL of $\text{CuSO}_4 \cdot 5\text{H}_2\text{O}$ (5 mM), 0.5 mL of sodium ascorbate (10 mM), and 0.25 mL of N_3 -PEG7-GRGDS (2 mM). The propargyl functionalized coverslips were inverted over a solution (80 μL) of the Click reagent and allowed to react for 4 h. After the reaction, the coverslips were profusely washed with deionized water, 20 mM EDTA solution, and again with water.

For ATR spectroscopy of the peptide functionalized films, the procedure described above was followed except that the functionalization was done on solvent cast films of the polymers.

For the preparation of polymer coated coverslips functionalized with Alexafluor 488, the same procedure as described above was followed except that in place of the peptide, N_3 -Alexafluor 488 was used.

Protein Adsorption. Gold quartz crystals (QX 301, Q-Sense AB) were spin-coated as described previously and mounted in stainless steel flow modules. Temperature control was set to 37 °C and samples were equilibrated in phosphate-buffered saline (PBS) before protein adsorption experiments. A 10% v/v bovine serum (FBS) was flowed through the modules at 24.2 $\mu\text{L}/\text{min}$ for 2 h. After the adsorption step, PBS was reintroduced through the system to remove any reversibly adsorbed protein. For selected materials, individual protein solutions, fibrinogen (Fg.) and bovine serum albumin (BSA) were adsorbed for 2 h at a concentration of 3 mg/mL.

Raw QCM-D data was modeled using manufacturer supplied software (Q-Tools, Q-Sense AB). Curve fitting using the Voigt model was performed by fixing fluid density, fluid viscosity, and layer density at 1000 kg/m³, 0.001 kg/ms, and 1200 kg/m³, respectively. Layer viscosity, layer shear, and layer thickness were fitted with limits of 10^{-6} – 10^{-2} kg/ms, 10^3 – 10^9 Pa, and 10^{-10} – 10^{-7} m, respectively, until a minimum χ^2 fit was obtained. Limits were varied through trial and error to determine whether χ^2 could be further minimized.

Cell Attachment. Polymer spin-coated coverslips were hydrated in PBS for 1 h at room temperature and subsequently seeded with NIH-3T3 cells at a density of 8000 cells/cm² in culture medium (88% DMEM supplemented with 10% bovine serum, 1% glutamine, and 1% penicillin-streptomycin). Following a 12 h attachment period, the coverslips were washed with PBS, and the adherent cell fraction removed by trypsinization. Trypsinized cells were pelleted by centrifugation and stored at –80 °C. Cell pellets were then assayed using Cyquant per the manufacturer's protocol (Invitrogen, Carlsbad, CA).

Cell Proliferation [w/o and w/RGD]. NIH-3T3 cells were G₀-synchronized at confluence by serum starvation (0.5%) for 72 h. Cells were then seeded on polymer spin-coated coverslips with or without GRGDS functionalization in serum-replete (10%) medium and incubated for 18 h. Cells were then pulsed with 5-ethynyl-2'-deoxyuridine (EdU, 5 mM) for an additional 8 h. Following the EdU pulse, cells were fixed in 4% paraformaldehyde and assayed using the Click-iT EdU proliferation kit (Invitrogen, Carlsbad, CA), according to the manufacturer's protocol. Nuclei were counterstained using DAPI, and cells were counted using epifluorescence imaging on a Nikon TE200 microscope.

Cell Differentiation. hMSCs (Lonza, Walkersville, MD) were seeded on polymer spin-coated coverslips with or without GRGDS functionalization at 12000 cells/cm² in basal growth medium (low glucose DMEM supplemented with 10% fetal bovine serum and 1% L-glutamine). Following an overnight attachment period, the medium was changed to a bone-fat bipotential differentiation medium (50% osteogenic, 50% adipogenic induction media, Lonza), and cells were cultured for an additional two weeks. At the end of the induction period, RNA was extracted (RNeasy kit, Qiagen) and converted to cDNA using reverse transcriptase (High Capacity Reverse Transcriptase kit, Applied Biosystems). Lineage marker gene expression was evaluated by

qPCR using Taqman assays (Applied Biosystems) on an ABI 7300 thermocycler. Gene expression in each condition was normalized to an internal control (RPLP0) and then further normalized to the expression level of bone or fat lineage markers observed on uncoated glass coverslips.

Scaffold Preparation. NaCl (11 g) was taken in a Teflon dish (6 cm diam) and packed by gentle tapping. The polymer H25N50G25 (0.22 g) was dissolved in 2.0 mL of dioxane and H₂O (0.22 mL) was added to this solution after the polymer dissolved and then poured evenly over the salt. The polymer–salt composition was mixed gently to homogenize the mixture, covered, and allowed to settle for 30 min. The mold with the polymer mixture was quenched in liquid N₂ (5 min) and the mixture (still in the mold) was lyophilized. The desired size of scaffold was punched out with a biopsy punch and then the scaffolds were immersed in water to leach out the salt. The water was refreshed until a solution of AgNO₃ showed no cloudiness indicating the absence of chloride salts. The scaffolds were then dried under vacuum for 3 days prior to characterization of pore architecture by SEM.

Results and Discussion

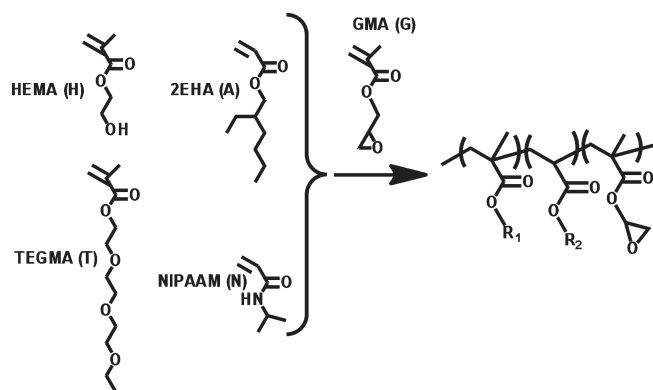
Synthesis and Characterization of Polymer Library. Here we describe the development of a focused library that spans a range of physical properties for the study of cell attachment, cell proliferation, and cell differentiation. The selection of monomers was designed such that their modulus and hydrophobic or hydrophilic nature would span a wide range and would also have a functional group for efficient surface modification with cell adhesion promoting peptides. Monomers with ionic functionalities were avoided since the properties of such polymers would over-ride the influences of the other monomers. With these parameters, the following monomers were selected: TEGMA (provides low modulus polymers), EHA (provides hydrophobic polymers), HEMA and NIPAAM (provides hydrophilic polymers), and GMA (provides the functional group for surface modification).

This focused library of 12 polymers was synthesized by AIBN-initiated radical polymerization of five monomers: HEMA, TEGMA, EHA, NIPAAM, and GMA. Glycidyl methacrylate was present in all the polymers at 25 mol % and the reactivity of the epoxide of GMA enables surface functionalization of these polymers. Four different families of polymers were synthesized by the combination of two of the above monomers and glycidyl methacrylate (Scheme 1). Subsequent variations of each family were obtained by varying the ratio of these two monomers while holding the concentration of GMA constant. By this methodology a correlated library of 12 polymers was synthesized.

Characterization of the polymers by NMR spectroscopy showed that the obtained composition was close to the feed composition. Although the obtained composition varies from the feed, the desired variations in feed compositions were maintained across the library (Table 1) and therefore the observed cellular responses can be correlated to changes in the polymer composition.

The static contact angles were determined on spin-coated polymer films on glass coverslips. Polymers containing EHA had higher contact angles compared to polymers containing HEMA or NIPAAM. In addition, variations in the chemical composition were reflected in the contact angles of these polymers. For example, a change in composition of the polymers from A55H20G25 to A25H50G25 resulted in a decrease in contact angle from 94 to 75° as a result of the increase of the hydrophilic component (HEMA) in the polymers. The T_g of the TEGMA containing polymers were low, consistent with the flexible nature of the ethylene glycol chain. Polymers containing both TEGMA and EHA had the lowest T_g .

Scheme 1. The Focused Library of Methacrylate Polymers Were Synthesized by AIBN Initiated Radical Polymerization^a



^a Each terpolymer was synthesized from a combination of GMA and any two of the four monomers HEMA, TEGMA, 2EHA, or NIPAAm.

The tensile moduli of these materials were determined from hydrated films (100 μm thick) of solvent cast polymers. Since these materials were being evaluated for their effect on cellular functions, it was more relevant to measure the wet modulus. The modulus measurements were calculated from the stress-strain curves at 2% strain. The tensile modulus of the materials varied between 30 and 3500 kPa. Polymers made from TEGMA were comparatively softer polymers. Polymers having high amounts of EHA did not soften after hydration, as expected from the hydrophobic nature of this monomer. On the other hand, HEMA-containing polymers softened upon hydration. Although the range of moduli in this library did not extend to the 0.1 to 30 kPa regime that is typically associated with modulus-dependent changes of cell behaviors,^{11,19} we tabulated these mechanical effects because they may be important to consider in applications with mechanical requirements and because it remained a possibility that this higher range of moduli might still have a cellular effect. The absence of interchain cross-links in our system precluded the ability to achieve the softer moduli obtained with hydrogel systems such as those made from polyacrylamide or polyethylene glycol wherein the hydrophilic polymer fraction typically accounts for less than 5% of the total mass.²⁰

Since topographical features can affect cell behavior,²¹ in the current work the polymers were fabricated as spin-coated films on glass coverslips. This is a commonly used procedure to examine cell behavior on polymeric surfaces and provides homogeneous thin films of ~ 100 nm thickness with minimum surface features,²² therefore minimizing the effect of topographical cues for the attached cells.

Cell Attachment. The attachment behavior of cells on polymeric surfaces is an important indicator of cell viability and subsequent proliferation and suitability of the polymer for

biomedical applications.²³ In the current study, the attachment of NIH 3T3 cells was evaluated on polymer films spin coated on glass coverslips. The cells were plated at a density of 8000 cells/ cm^2 and allowed to attach for 12 h prior to trypsinization. Cell numbers were quantified based on DNA content, using Cyquant dye. A large variation in cell attachment across the polymer library was observed (Table 1). In general, hydrophobic polymers (those with EHA) showed high cell attachment whereas the hydrophilic polymers (those with HEMA/NIPAAm) showed low cell attachment, demonstrating that this polymer library affords the potential for a wide range of cell attachment properties. We also confirmed no correlation between substrate stiffness and cell attachment (data not shown), consistent with our earlier measurements that the range of moduli spanned by this library was not biologically active. Such libraries of well-defined chemical compositions have applicability in the combinatorial development of surfaces that support cell adhesion and proliferation of desired cell populations.

Protein Adsorption. Since the adsorption of adhesive proteins to the polymer surface precedes cell attachment,²⁴ it was hypothesized that differential protein adsorption on the various polymer surfaces accounted for the observed variability in cell attachment across the polymer library. To test this possibility, the amount of protein adsorption to the polymers (quartz crystal microbalance with dissipation technique (QCM-D)²⁵) was assayed using fibrinogen (Fg), a 340 kDa protein, commonly studied in the context of blood-contacting biomaterials. The QCM-D results (Figure 1) showed a trend similar to that of cell attachment with more Fg adsorption seen on hydrophobic polymers than on the hydrophilic polymers (see also Supporting Information S1). Similar to PEG, it is likely that interactions between HEMA and water molecules repel proteins, which in turn causes low cell attachment. Bovine serum albumin (65 kDa), the most abundant protein in serum, also showed similar behavior to Fg. In contrast, when 10% serum was used in lieu of Fg or BSA, all polymers exhibited similar levels of protein adsorption. While total adsorption of serum proteins may be grossly similar across these polymers, it is likely that polymer composition influences the competitive adsorption of proteins that specifically promote adhesion (such as Fg) versus noncell adhesive ones (such as BSA), or that polymers with low attachment potential may selectively adsorb adhesive proteins in nonfunctional conformations.²⁶

Cell Proliferation. We next examined the impact of polymer composition on cell proliferation. The 3T3 cells were G_0 -synchronized and allowed to attach for 26 h. Cell proliferation was measured as a function of S-phase entry by assaying for cellular incorporation of the nucleotide analog, EdU (5-ethynyl-2'-deoxyuridine). The fraction of EdU-positive cells was used to compute a proliferation index (% proliferation) for the population of cells that successfully attach to the polymers. The results (Table 1) show that cell proliferation depends on polymer chemistry. Polymers composed of EHA robustly supported cell proliferation, whereas the hydrophilic polymers (those with HEMA or NIPAAm) antagonized the proliferation of 3T3 cells. This effect of chemistry on proliferative response was qualitatively similar to that seen for

(19) Guo, W. H.; Frey, M. T.; Burnham, N. A.; Wang, Y. L. Substrate rigidity regulates the formation and maintenance of tissues. *Biophys. J.* **2006**, *90*(6), 2213–20.

(20) Yeung, T.; Georges, P. C.; Flanagan, L. A.; Marg, B.; Ortiz, M.; Funaki, M.; Zahir, N.; Ming, W.; Weaver, V.; Janney, P. A. Effects of substrate stiffness on cell morphology, cytoskeletal structure, and adhesion. *Cell Motil. Cytoskeleton* **2005**, *60*(1), 24–34.

(21) Lim, J. Y.; Donahue, H. J. Cell sensing and response to micro- and nanostructured surfaces produced by chemical and topographic patterning. *Tissue Eng.* **2007**, *13*(8), 1879–91.

(22) Karp, J. M.; Shoichet, M. S.; Davies, J. E. Bone formation on two-dimensional poly(DL-lactide-co-glycolide) (PLGA) films and three-dimensional PLGA tissue engineering scaffolds in vitro. *J. Biomed. Mater. Res. A* **2003**, *64*(2), 388–96.

(23) Anselme, K. Osteoblast adhesion on biomaterials. *Biomaterials* **2000**, *21*(7), 667–81.

(24) Andrade, J. D.; Hlady, V. Protein Adsorption and Materials Biocompatibility - a Tutorial Review and Suggested Hypotheses. *Adv. Polym. Sci.* **1986**, *79*, 1–63.

(25) Le Guillou-Buffello, D.; Helary, G.; Gindre, M.; Pavon-Djavid, G.; Laugier, P.; Migonney, V. Monitoring cell adhesion processes on bioactive polymers with the quartz crystal resonator technique. *Biomaterials* **2005**, *26*(19), 4197–205.

(26) Sivaraman, B.; Fears, K. P.; Latour, R. A. Investigation of the Effects of Surface Chemistry and Solution Concentration on the Conformation of Adsorbed Proteins Using an Improved Circular Dichroism Method. *Langmuir* **2009**, *25*(5), 3050–6.

Table 1. Chemical, Physical, and Biological Properties of the Library of Polymers

composition		contact angle	cell number (cell attachment)	% proliferation	modulus (kPa)	T_g (°C)
feed	from NMR					
A55T20G25	A62T14G23	96 ± 1.28	11998 ± 5818	85 ± 1.61	32 ± 19	−37
A40T35G25	A42T27G31	92 ± 1.83	11975 ± 500	78 ± 5.01	37 ± 15	−37
A10T65G25	A18T53G29	85 ± 2.77	8350 ± 585	40 ± 6.49	39 ± 19	−41
H40T35G25	H35T37G28	75 ± 2.27	210 ± 123	27 ± 2.28	354 ± 36	−5
H25T50G25	H24T50G26	69 ± 1.88	406 ± 33	28 ± 9.86	157 ± 6	−3
H10T65G25	H13T59G28	72 ± 1.34	618 ± 304	41 ± 10.13	52 ± 5	−28
A55H20G25	A52H20G27	94 ± 1.65	5402 ± 4971	78 ± 3.08	1275 ± 205	15
A40H35G25	A37H36G27	82 ± 2.78	6486 ± 2613	59 ± 18.8	3380 ± 141	37
A25H50G25	A26H51G23	75 ± 2.37	1843 ± 1902	29 ± 9.27	2697 ± 704	68
H40N35G25	H36N40G24	61 ± 2.37	363 ± 66	24 ± 3.06	2280 ^a	138
H25N50G25	H22N49G29	65 ± 1.08	831 ± 60	8 ± 3.3	1850 ^a	119
H10N65G25	H14N57G29	64 ± 1.48	1208 ± 326	16 ± 9.45	1150 ^a	119

^a The standard deviation for the H-N-G series of polymers could not be obtained due to the difficulty in preparing pressed films of this series of polymers.

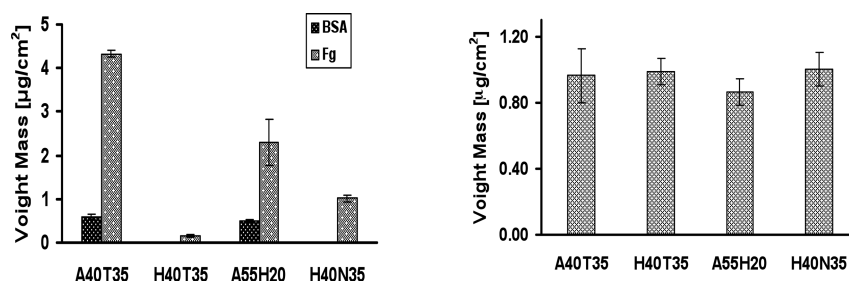


Figure 1. Differential adsorption of fibrinogen (Fg) and bovine serum albumin (BSA) (left) onto polymer-coated surfaces, as determined by QCMD. The hydrophobic polymers (A40T35, A55H20) adsorb more Fg or BSA than hydrophilic polymers (H40T35, H40N35). Adsorption of serum proteins onto polymer coated surfaces (right). (For simplicity, polymer nomenclature in all figures omits reference to the amount of glycidyl methacrylate (G), which is a constant 25 mol % across the library. Error bars indicate standard deviations.)

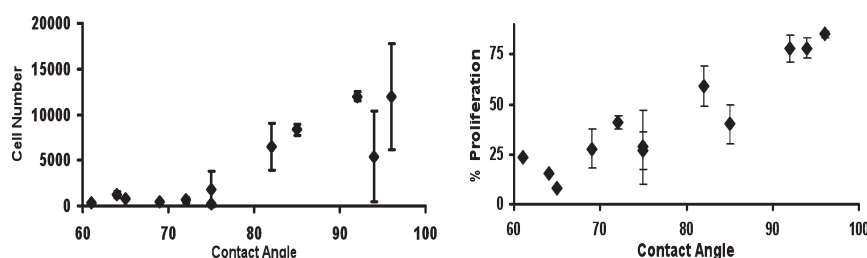


Figure 2. Correlation plots of contact angle of the polymers with either cell attachment (left) or proliferation (right) of NIH 3T3 fibroblasts. Both cell attachment and proliferation of NIH 3T3 cells are enhanced on hydrophobic surfaces compared to hydrophilic surfaces. (Error bars are standard deviations.)

cell attachment on these polymers. Indeed, this material-dependent cell attachment and proliferation followed the trends in contact angles. High cell attachment and proliferation was seen in polymers having high contact angles and those with low contact angles had low attachment and proliferation (Figure 2). Again, there was no correlation between the cell proliferation behavior and the modulus of the materials. For example, polymers A40T35G25 and A55H20G25 had very high proliferation while having very different tensile moduli. On the other hand, polymers A55H20G25 and H10N65G25 were in the same modulus range but exhibited very different proliferation behavior. Taken together, the observations suggest that poor adsorption of ECM proteins to HEMA or NIPAAm rich surfaces limits the ability of cells to adhere to the surface, and this low adhesion context attenuates the adhesion-based signaling that is required for efficient proliferation in response to serum mitogens. Alternatively, changes in the conformation of ECM proteins adsorbed to HEMA or NIPAAm surfaces may render them deficient for activation of integrins.

Surface Functionalization with Adhesive Peptides. Without controlling for cell adhesion of the polymers, cell behavior on thin polymer films in the terpolymer library was strongly influenced by the substrate chemistry. To test the cumulative effect of cell adhesive peptides and polymer chemistry on cell functions, the polymer surfaces were functionalized with adhesive peptides. To guarantee that coupling of adhesive peptides could occur independently of the hydrophobicity of the polymers, a highly efficient peptide-coupling reaction was required. To achieve this aim, we used a two-step process. First, the surface epoxides of GMA were converted to propargyl groups via reaction with propargyl amine. Second, the propargyl groups were covalently coupled to an azide terminated PEG7-GRGDS peptide using Huisgen 1,3-cycloaddition reaction (Sharpless Click reaction).²⁷ The GRGDS peptide was linked to the azide through a PEG spacer having seven

(27) Lutz, J. F.; Zarafshani, Z. Efficient construction of therapeutics, bioconjugates, biomaterials and bioactive surfaces using azide-alkyne “click” chemistry. *Adv. Drug. Delivery Rev.* **2008**, *60*(9), 958–70.

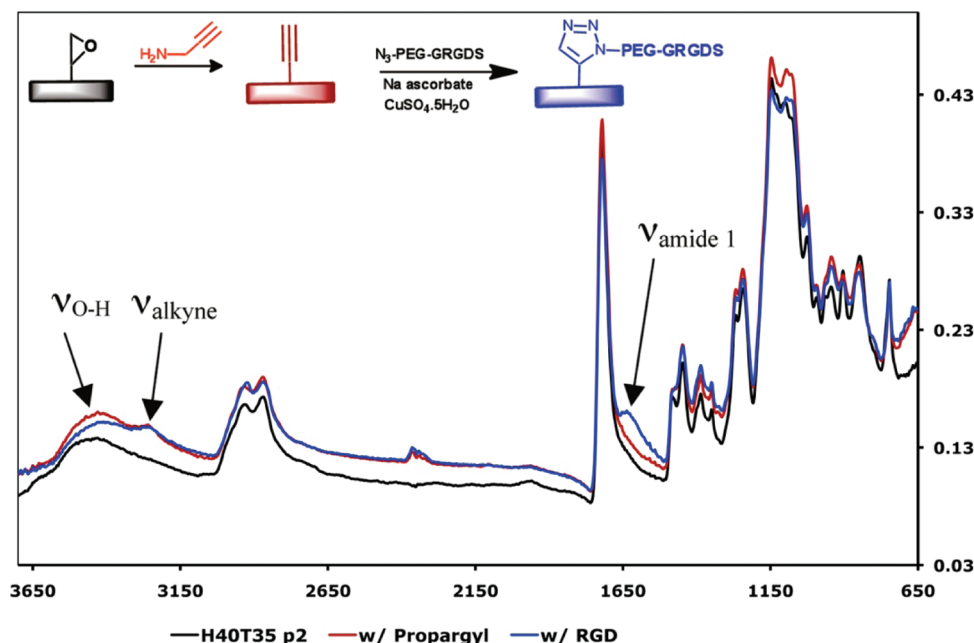


Figure 3. ATR-FTIR spectra of unfunctionalized H40T35G25 polymer (black); the same polymer surface-functionalized with propargyl groups (brown) showing the presence of alkyne peaks (3266 cm^{-1}); and with surface GRGDS peptide (blue) showing the presence of the amide I band (1645 cm^{-1}).

ethylene glycol units. The need for a spacer to increase cell attachment has been demonstrated previously and a distance of 11–46 Å is considered to be ideal for improved cell attachment.²⁸

Surface functionalization with GRGDS peptide was verified by ATR-FTIR spectroscopy on a solvent cast film of the polymer. Peaks corresponding to the alkyne and the amide I peak of the peptide confirm the success of the surface functionalization strategy. The peak at 3266 cm^{-1} corresponds to the alkyne C–H stretch²⁹ and the peak at 1645 cm^{-1} corresponds to the amide I band³⁰ (Figure 3).

To demonstrate that the surface functionalization was efficient across the library, we monitored the coupling reaction using an azide terminated Alexafluor 488 dye. Supporting Information Figure S2 shows the intensity of fluorescence from surface functionalized spin coated polymer films. The intensity of fluorescence is slightly higher in the hydrophilic polymers (those with HEMA or NIPAAm) compared to the hydrophobic polymers (those with EHA). Nevertheless the fluorescence does not vary widely between these two groups. In addition, the reproducibility of the method is illustrated by the similar fluorescence intensities from two coverslips of the same polymer. This functionalization strategy offers advantages over other commonly used methods, such as activation of a carboxylic acid with EDC or NHS. The reactive intermediates of these reactions are subject to hydrolysis and to nonproductive side-reactions such as formation of *N*-acylurea in polar solvents.³¹

As expected, peptide functionalization of the polymer surfaces causes a reduction of the contact angles of these materials (Figure 4).

(28) Beer, J. H.; Springer, K. T.; Collier, B. S. Immobilized Arg-Gly-Asp (RGD) peptides of varying lengths as structural probes of the platelet glycoprotein IIb/IIIa receptor. *Blood* **1992**, 79(1), 117–28.

(29) De Geest, B. G.; Van Camp, W.; Du Prez, F. E.; De Smedt, S. C.; Demeester, J.; Hennink, W. E. Biodegradable microcapsules designed via “click” chemistry. *Chem. Commun. (Cambridge, U.K.)* **2008**, 2, 190–2.

(30) Larsen, C. C.; Kligman, F.; Kottke-Marchant, K.; Marchant, R. E. The effect of RGD fluorosurfactant polymer modification of ePTFE on endothelial cell adhesion, growth, and function. *Biomaterials* **2006**, 27(28), 4846–55.

(31) Nakajima, N.; Ikada, Y. Mechanism of Amide Formation by Carbodiimide for Bioconjugation in Aqueous Media. *Bioconjug. Chem.* **1995**, 6(1), 123–30.

In all the polymers except the EHA-TEGMA-GMA series there is an appreciable decrease in the contact angles with GRGDS functionalization. There is almost a 20° change in contact angle after surface functionalization (average contact angle before and after functionalization = 61 and 78° respectively). The EHA-TEGMA-GMA is the most hydrophobic series of polymers in the library and the surface functionalization with peptides does not compensate for the inherent hydrophobicity of these polymeric surfaces.

Cell Attachment on Surfaces with GRGDS Peptides. The tripeptide sequence RGD is a surrogate for fibronectin and is sufficient to induce cell attachment to polymer surfaces. In the current work, attachment of NIH 3T3 cells was examined on the library of polymers that had been surface modified with the adhesive peptide GRGDS having a PEG spacer. The effect of the GRGDS peptide on cell attachment is shown in Figure 5. Without peptides, cell attachment was substantially higher in polymers containing EHA (the hydrophobic polymers) while the hydrophilic polymers resisted cell attachment. Conversely, in the presence of surface peptides, cell attachment was equalized across all the polymers, overriding the influence of the substrate chemistry.

As a control for the specificity of the increased cell attachment response to the GRGDS peptide, we assayed cell attachment on polymers coupled to an azide-terminated PEG (Figure 6). Cell attachment remained low for the hydrophilic polymers with or without PEG. However, PEG-functionalization almost completely decreased the cell attachment on the EHA-HEMA-GMA polymers while it decreased the attachment by about 40% on the EHA-TEGMA-GMA surfaces.

Cell Proliferation on Surfaces with GRGDS Peptides. GRGDS functionalized polymers were subsequently characterized for cell proliferation responses. Similar to the cell attachment response, the proliferation rates are normalized across all the polymers functionalized with GRGDS, and in fact, the functionalized polymers exhibited maximal cell proliferation potential (Figure 7). Therefore the presence of RGD peptides overrides the influence of the chemistry of the materials.

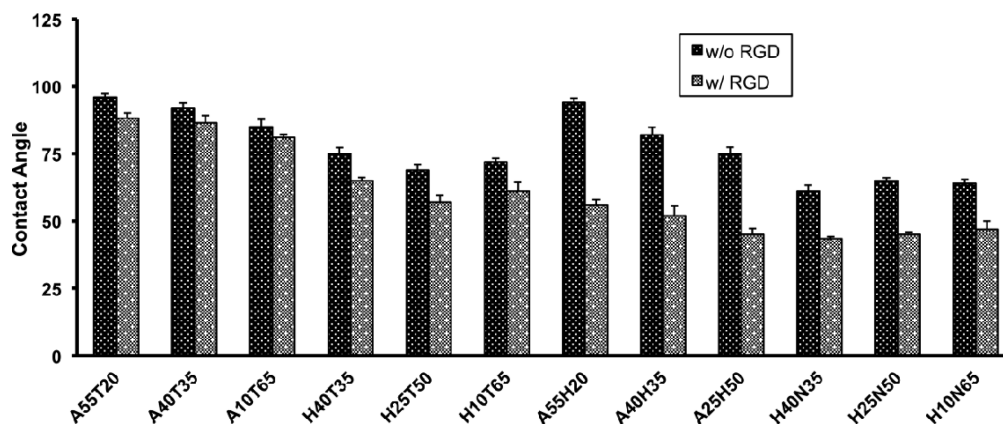


Figure 4. Effect of surface functionalization with GRGDS peptide on contact angle. In all the polymers except the A-T-G series there is an appreciable decrease in the contact angles with GRGDS functionalization (lighter bars) as compared to the nonfunctionalized polymer (darker bars). (Error bars indicate standard deviations.)

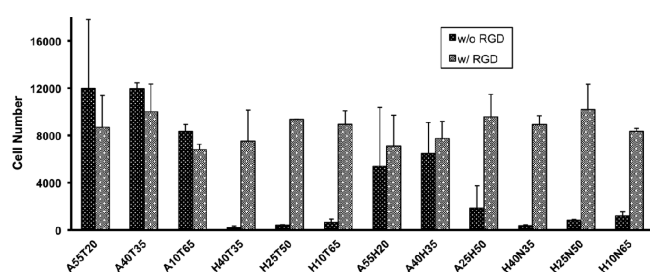


Figure 5. NIH-3T3 cell attachment on nonfunctionalized and GRGDS functionalized surfaces in serum-replete medium (DMEM + 10% bovine serum). In the presence of surface peptides, cell attachment was equalized across all the polymers, overriding the influence of the substrate chemistry. (Error bars indicate standard deviations.)

Although RGD functionalization has been shown to improve cell attachment and proliferation numerous times in the literature, to the best of our knowledge this is the first demonstration of the normalization of cell attachment and proliferation across a number of polymers after RGD functionalization. This observation is significant to biomaterials design since it illustrates that in principle a polymer selected for specific material properties, but deficient in cellular responses, can be rescued for biological functionality by efficient coupling of a cell-adhesive peptide.

hMSC Differentiation. It has been postulated that stem cell differentiation can be controlled by the properties of biomaterial or polymeric substrates.^{32,33} In fact, small changes in material chemistry can bring about significant differences in lineage commitment as shown in a methacrylate polymer gel system with different pendant functional groups.³⁴ However very little is known of how material composition might influence MSC differentiation, partly due to a lack of a variety of materials examined. We therefore examined the differentiation of human mesenchymal stem cells on our polymer library with and without GRGDS peptides. The results showed that the chemistry of the polymers modulated osteogenic differentiation of the MSCs as indicated by the expression levels of alkaline phosphatase (ALP), an early stage bone marker (Figure 8). A40H35G25, a hydrophobic polymer,

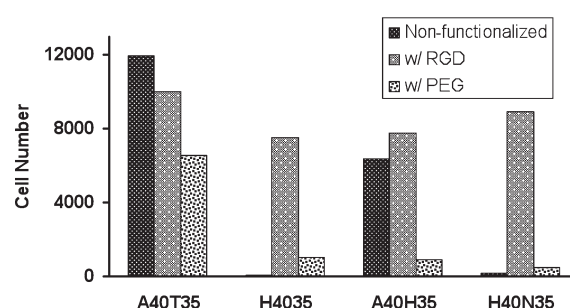


Figure 6. NIH-3T3 cell attachment on nonfunctionalized, GRGDS-functionalized, and PEG-functionalized surfaces in serum-replete medium (DMEM + 10% bovine serum). Attachment of PEG to the hydrophobic A40T35 and A40H35 polymers decreases cell attachment, likely by preventing adsorption of serum proteins that promote cell-adhesion. Additionally, cell attachment remains low on the hydrophilic surfaces with PEG, demonstrating that increasing the cell adhesion of these polymers requires the presence of the GRGDS sequence, specifically.

induced the highest expression levels of ALP. ALP expression on this polymer is substantially higher than the glass control. As in the proliferation experiments, the presence of GRGDS peptides overrode the influence of chemical composition in the library of polymers. That is, in the presence of GRGDS peptides the expression of ALP was normalized across the polymers examined. Similarly, the expression of LPL, a fat marker, was also normalized on surfaces having GRGDS peptides (Figure 8). While the nature of the RGD dependent effects on MSC differentiation warrant further study, it is clear that increasing the cell adhesion of these polymers is favorable for the differentiation process. Moreover, it may suggest a useful avenue to tune the differentiation response of cells, particularly when biomaterial design principles that require specific chemistries lie orthogonal to the desired differentiation outcome.

Fabrication of Porogen-Leached Scaffolds. It was shown above that the cell response to materials can be modulated by surface peptides irrespective of the substrate chemistry. However, only polymers with the appropriate material properties can be fabricated into devices such as scaffolds. Porogen-leached or

(32) Lutolf, M. P.; Gilbert, P. M.; Blau, H. M. Designing materials to direct stem-cell fate. *Nature* **2009**, 462(7272), 433–41.

(33) Saha, K.; Pollock, J. F.; Schaffer, D. V.; Healy, K. E. Designing synthetic materials to control stem cell phenotype. *Curr. Opin. Chem. Biol.* **2007**, 11(4), 381–387.

(34) Benoit, D. S. W.; Schwartz, M. P.; Durney, A. R.; Anseth, K. S. Small functional groups for controlled differentiation of hydrogel-encapsulated human mesenchymal stem cells. *Nat. Mater.* **2008**, 7(10), 816–823.

(35) Lee, J.; Cuddihy, M. J.; Kotov, N. A. Three-dimensional cell culture matrices: state of the art. *Tissue Eng., Part B Rev* **2008**, 14(1), 61–86.

(36) Pham, Q. P.; Sharma, U.; Mikos, A. G. Electrospinning of polymeric nanofibers for tissue engineering applications: a review. *Tissue Eng.* **2006**, 12(5), 1197–211.

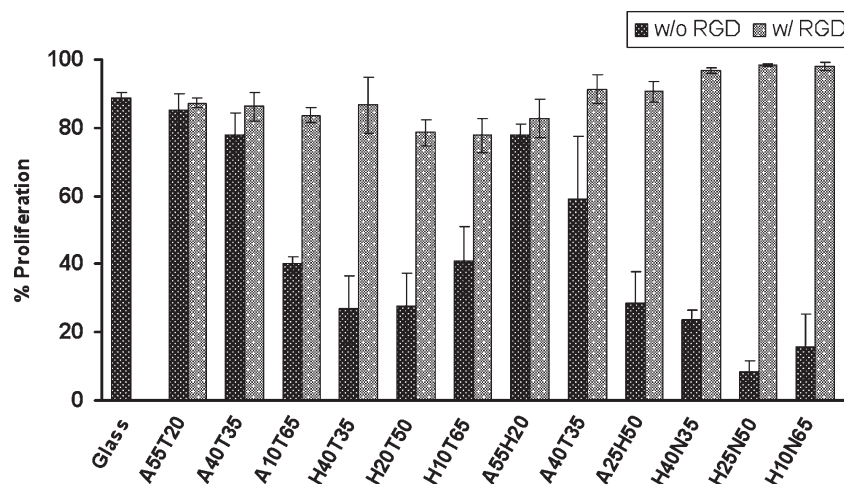


Figure 7. NIH-3T3 cell proliferation on the library of polymers with and without surface-functionalized GRGDS peptides in serum-replete medium (DMEM + 10% bovine serum). In the presence of surface peptides, cell attachment was equalized across all the polymers, overriding the influence of the substrate chemistry. (Error bars indicate standard deviations.)

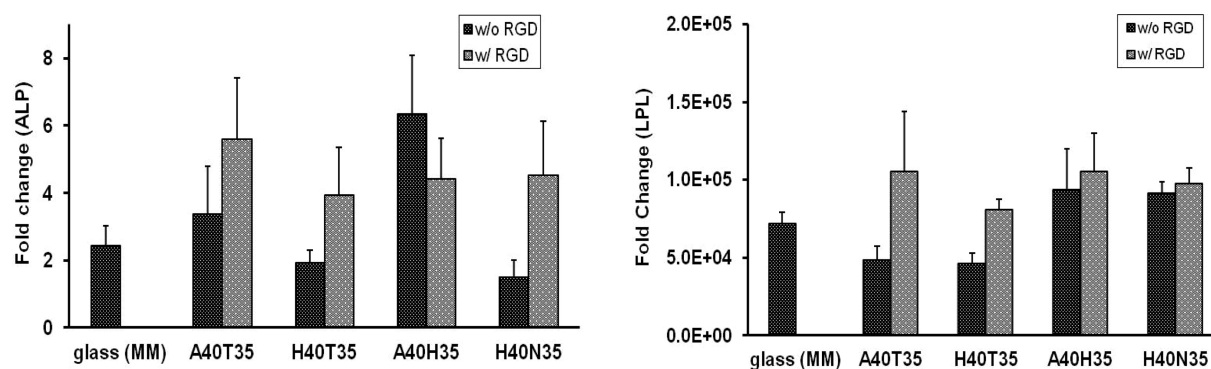


Figure 8. Expression of alkaline phosphatase (ALP) (left) and lipoprotein lipase (LPL) (right) on a subset of the library of polymers as a function of hMSC differentiation. In the absence of surface peptides, the expression of both ALP and LPL is dependent upon the chemistry of the substrate. However upon surface functionalization with GRGDS peptides, the expression of ALP and LPL is normalized across the polymers. (Error bars indicate standard deviations.)

gas-foamed scaffolds³⁵ and electrospun mats³⁶ are increasingly used to provide a three-dimensional (3D) environment for cellular growth and proliferation. Such 3D matrices are a closer representation of the cell microenvironment. Materials for scaffolds and electrospun mats should have a sufficiently high modulus so that the structural integrity is maintained after fabrication. The polymer H40N35G25 has a modulus of 2280 kPa and without surface peptides showed lower ALP expression. SEM images of porogen-leached scaffolds prepared from this polymer exhibit macroporous and microporous architecture (Supporting Information S3). From the studies on polymer films of this material, it is indicated that functionalization of the scaffold with RGD peptides could improve the expression of ALP. Such studies are currently underway in our laboratories. Similar scaffolds were fabricated from the A40H35G25 polymer, which also showed good macroporous and microporous architecture (Supporting Information S3).

Conclusions

A focused library of materials was synthesized from commercially available methacrylate or acrylate monomers. This relatively small library of polymers has a wide variation in properties, such as the contact angle and modulus, and these properties can be tuned by varying the composition of the

polymers. The design of the library also enables the efficient surface functionalization with biologically active peptides. Such a tunable library allows the examination of how systematic changes in material composition affect biological responses such as protein adsorption and cell attachment, proliferation, and differentiation.

The work described shows that in the absence of surface peptides, the composition of the polymers can influence cell behavior with the strongest correlation between contact angle, protein adsorption, and cell response. However, immobilizing an adhesive peptide to the surface of the polymers overrides the inherent attachment, proliferation, and differentiation profiles of the underlying polymer composition. This is the first demonstration of enhanced cellular responses upon surface functionalization with peptides across a whole library of materials and this observation has important implications for the design of biomaterials.

The work also shows that some of the polymers developed here can be fabricated into porogen leached scaffolds. Such scaffolds, which can be efficiently surface functionalized with peptides, may be useful 3D matrices for cell culture.

Acknowledgment. This work was supported by RESBIO (Integrated Technology Resource for Polymeric Biomaterials) funded by the National Institutes of Health (NIBIB and NCMHD)

under Grant P41 EB001046. The content is solely the responsibility of the authors and does not necessarily represent the official views of the NIH, NIBIB, or NCMHD. An NIH T32 postdoctoral fellowship for A.J. is gratefully acknowledged (Grant T32EB005583 from the National Institute of Biomedical Imaging And Bioengineering).

The authors thank Professor Gene Hall for the use of his ATR-FTIR spectrophotometer.

Supporting Information Available: Additional figures. This material is available free of charge via the Internet at <http://pubs.acs.org>.